

## MIT Open Access Articles

*Controlled release of functional proteins through designer self-assembling peptide nanofiber hydrogel scaffold*

The MIT Faculty has made this article openly available. **Please share** how this access benefits you. Your story matters.

**Citation:** Koutsopoulos, Sotirios et al. "Controlled release of functional proteins through designer self-assembling peptide nanofiber hydrogel scaffold." Proceedings of the National Academy of Sciences 106.12 (2009): 4623-4628.

**As Published:** <http://dx.doi.org/10.1073/pnas.0807506106>

**Publisher:** National Academy of Sciences

**Persistent URL:** <http://hdl.handle.net/1721.1/50253>

**Version:** Final published version: final published article, as it appeared in a journal, conference proceedings, or other formally published context

**Terms of Use:** Article is made available in accordance with the publisher's policy and may be subject to US copyright law. Please refer to the publisher's site for terms of use.



# Controlled release of functional proteins through designer self-assembling peptide nanofiber hydrogel scaffold

Sotirios Koutsopoulos<sup>a,1</sup>, Larry D. Unsworth<sup>a,b,c</sup>, Yusuke Nagai<sup>a,d</sup>, and Shuguang Zhang<sup>a,1</sup>

<sup>a</sup>Center for Biomedical Engineering, Massachusetts Institute of Technology, 77 Massachusetts Avenue, Cambridge, MA 02139; <sup>b</sup>National Research Council, National Institute for Nanotechnology, 11421 Saskatchewan Drive, Edmonton, AB, Canada T6G 2M9; <sup>c</sup>Department of Chemical and Materials Engineering, University of Alberta, Edmonton, AB, Canada T6G 2G6; and <sup>d</sup>Menicon Co., Ltd., 5-1-10 Takamori-dai, Kasugai, Aichi 487-0032, Japan

Edited by Arnold L. Demain, Drew University, Madison, NJ, and approved February 6, 2009 (received for review July 31, 2008)

The release kinetics for a variety of proteins of a wide range of molecular mass, hydrodynamic radii, and isoelectric points through a nanofiber hydrogel scaffold consisting of designer self-assembling peptides were studied by using single-molecule fluorescence correlation spectroscopy (FCS). In contrast to classical diffusion experiments, the single-molecule approach allowed for the direct determination of diffusion coefficients for lysozyme, trypsin inhibitor, BSA, and IgG both inside the hydrogel and after being released into the solution. The results of the FCS analyses and the calculated pristine in-gel diffusion coefficients were compared with the values obtained from the Stokes–Einstein equation, Fickian diffusion models, and the literature. The release kinetics suggested that protein diffusion through nanofiber hydrogels depended primarily on the size of the protein. Protein diffusivities decreased, with increasing hydrogel nanofiber density providing a means of controlling the release kinetics. Secondary and tertiary structure analyses and biological assays of the released proteins showed that encapsulation and release did not affect the protein conformation and functionality. Our results show that this biocompatible and injectable designer self-assembling peptide hydrogel system may be useful as a carrier for therapeutic proteins for sustained release applications.

drug delivery | protein diffusion | single-molecule analysis | spectroscopic analyses | antibody–antigen interactions

Hydrogels have long been recognized as being well suited for numerous biomedical applications, including regenerative medicine and controlled drug release (1–3). The successful implementation of these materials, however, depends on many factors, including component and degradation product toxicity, inflammatory host response, the ease of incorporating cell-specific bioactive moieties, and the controlled and sustainable release of the active compound over prolonged periods of time. Despite the intense research conducted on myriad natural and synthetic materials (i.e., polyglycolic–polylactic acid, agarose, collagen, alginate, etc.), all of these challenges have not been resolved yet for a single system (2, 4).

In 1993, we discovered that a class of self-assembling peptides comprising alternating hydrophobic and hydrophilic amino acids spontaneously self-organize into interwoven nanofibers with diameters of 10–20 nm upon being introduced to electrolyte solutions (5). These nanofibers further organize to form highly hydrated hydrogels [up to  $\approx 99.5\%$  (wt/vol) water], with pore sizes between 5 and 200 nm in diameter. Peptide hydrogels not only have all of the advantages of “traditional” hydrogels but also do not use harmful materials (e.g., toxic cross-linkers, etc.) to initiate the solution–gel transformation (2) whereas the degradation products are natural amino acids, which can be metabolized. The fact that the solution–gel transition occurs at physiological conditions and the high internal hydration of the hydrogel allows for the presentation of bioactive molecules and/or cells that may be coinjected locally in a tissue-specific

manner. Self-assembling peptide hydrogel scaffolds are biocompatible, amenable to molecular design, and have been used in a number of tissue engineering applications, including bone and cartilage reconstruction, heart tissue regeneration, angiogenesis, and more (6–8). Peptide hydrogels provide a platform that makes them ideal for nanomedical applications because they are easy to use, nontoxic, nonimmunogenic, nonthrombogenic, biodegradable, and applicable to localized therapies through injection to a particular tissue (8, 9).

We reported that the acetyl-(Arg-Ala-Asp-Ala)<sub>4</sub>-CONH<sub>2</sub> [Ac-(RADA)<sub>4</sub>-CONH<sub>2</sub>] peptide hydrogel is an efficient slow-delivery carrier of small molecules (10). In this work, we used a variety of proteins, including lysozyme, trypsin inhibitor, BSA, and IgG with differing physicochemical properties (pI 4.6, 11.4; molecular mass, 14.3–150 kDa) and morphologies and encapsulated them within the Ac-(RADA)<sub>4</sub>-CONH<sub>2</sub> peptide hydrogel (Fig. 1). Release kinetics and diffusion coefficients for all systems were determined by using a single-molecule fluorescence correlation spectroscopy (FCS) method. In contrast to bulk experiments where average diffusion values are determined by using semiempirical approaches, the single-molecule approach allowed for the experimental determination of diffusion coefficients of the proteins not only in solution but also inside the hydrogel during the release process.

It is crucial to determine whether the processes involved in incorporating and releasing proteins from the peptide hydrogel adversely affect their structural conformation and function. To ascertain the released protein structure and function, these proteins were analyzed by using circular dichroism (CD) and fluorescent spectroscopy before and after release. Furthermore, bioassays were conducted to verify protein functionality. The presentation of functional proteins and the elucidation of crucial protein–hydrogel events are considered as significant advances that are required for furthering designer peptide nanofiber hydrogels for various biomedical applications.

## Results and Discussion

**Protein Release Through the Self-Assembling Peptide Hydrogel.** From Fig. 2, it is apparent that for these systems, there seemed to be a rapid initial release of protein within the 1st h (burst effect). This burst is most likely caused by (*i*) protein molecules that were at or near the solvent–hydrogel interface and escaped rapidly into the supernatant solution and (*ii*) protein release that is faster through large pores of the hydrogel compared with that through smaller pores and parts of the hydrogel with highly entangled nanofiber network that constrain the molecular motion.

Author contributions: S.K., L.D.U., Y.N., and S.Z. designed research; S.K., L.D.U., and Y.N. performed research; S.K., L.D.U., Y.N., and S.Z. analyzed data; and S.K., L.D.U., and S.Z. wrote the paper.

The authors declare no conflict of interest.

This article is a PNAS Direct Submission.

<sup>1</sup>To whom correspondence may be addressed. E-mail: sotiris@mit.edu or shuguang@mit.edu.

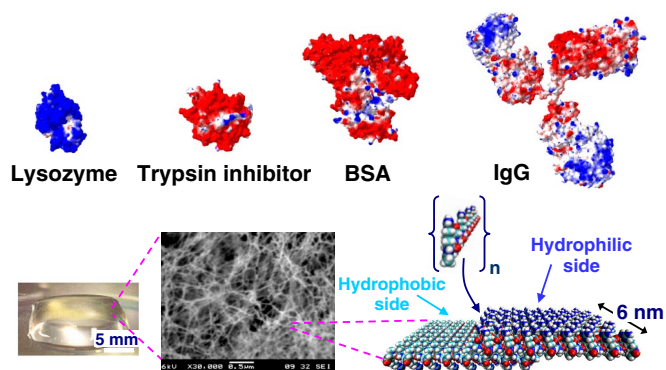


**Fig. 1.** Graphical representation of lysozyme, trypsin inhibitor, BSA, and IgG, the Ac-(RADA)<sub>4</sub>-CONH<sub>2</sub> peptide monomer, and of the peptide nanofiber. Color scheme for proteins and peptides: blue, positively charged; red, negatively charged; light blue, hydrophobic. Protein models were based on known crystal structures (37–40).

Protein release through the 1% (wt/vol) peptide hydrogel was slower by time and seemed to reach a plateau value asymptotically after  $\approx 30$ –50 h depending on the protein. In hydrogel systems, protein release rarely reaches 100%. The main reason for that is physical entrapment of the molecules in highly entangled nanofiber domains of the hydrogel, which allow less free motion of the diffusant. Because the self-assembling peptide hydrogel is biodegradable, upon introduction into a living organism, proteolytic enzymes will degrade the peptides and the hydrogel will be decomposed to single amino acids. This process will allow for the entire load of the hydrogel to be released into the host tissue. IgG presented the slowest release among the proteins tested, and its concentration in the supernatant was increasing even after 60 h of release. These results show that large proteins are retained inside the hydrogel scaffold for longer times compared with smaller proteins. Overall, it seems evident that protein release from the Ac-(RADA)<sub>4</sub>-CONH<sub>2</sub> peptide

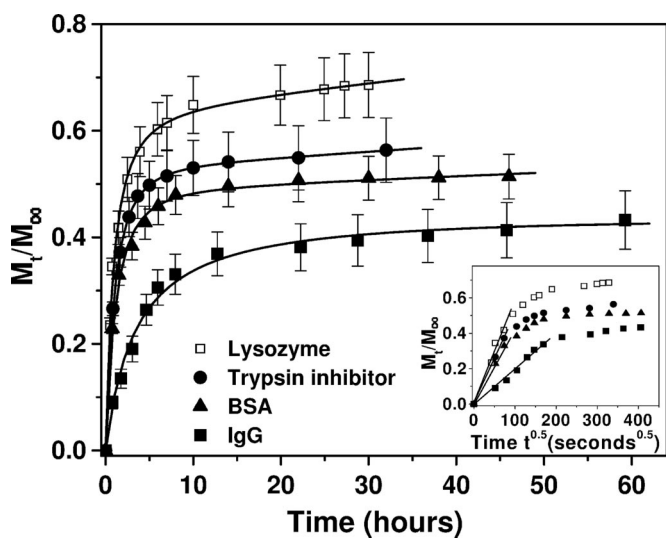


**Fig. 2.** Release profiles for lysozyme (□), trypsin inhibitor (●), BSA (▲), and IgG (■) through the self-assembling peptide hydrogel in PBS (pH 7.4) at room temperature. Data points represent the average of 4 or 8 samples with calculated SD values that are  $<12\%$ . (Inset) Protein release plotted as a function of the square root of time showing a biphasic diffusion mechanism. The initial linear part of the plots represents simple diffusion of the proteins through the peptide hydrogel, and it is used to calculate diffusion coefficients based on Fick's law (Eq. 2).

hydrogel was more sensitive to physical size than protein charge (Fig. 2). Lysozyme, which is the smallest among the proteins studied, was released fastest. Soybean trypsin inhibitor, which is slightly larger and oppositely charged compared with lysozyme, was released slower than lysozyme but faster than BSA, which is larger. IgG, the largest of the proteins examined, was released more slowly than all other proteins.

Theoretical calculations revealed that the isoelectric point of the Ac-(RADA)<sub>4</sub>-CONH<sub>2</sub> peptide is between 6.7 and 7.0, and therefore, it is suggested that at pH 7.4, where the protein release experiments were conducted, the net charge of the peptide nanofibers is only slightly negative. The release data show that at these conditions, the protein surface charge was not a significant factor dictating the diffusion mechanism. However, we can speculate that protein charge could be an important factor affecting the release kinetics when protein release occurred through peptide hydrogels consisting of nanofibers that carry a net (positive or negative) charge. Such peptide sequences with self-assembling properties can be easily designed and synthesized, and this strategy would present an efficient means to control the release profile of proteins through the hydrogel.

**Protein Diffusivity in Solution and in the Hydrogel Scaffold.** The release profiles of proteins with different molecular mass, isoelectric points, and hydrodynamic radii through the peptide nanofiber hydrogel system were studied by using a single-molecule FCS method. We measured the number of particles crossing the confocal volume,  $\approx 1$  fL, per unit of time and the diffusional time, which is the time required for the diffusing molecules to cross the confocal volume. The diffusion coefficients of the proteins were determined both in solution and inside the hydrogel (pristine), and the results are summarized in Table 1.

The results show that the Stokes–Einstein equation overestimates the diffusivities of the proteins in solution by 10–20%. The reason for the discrepancy between the Stokes–Einstein diffusion coefficients and those determined by FCS analysis is probably because in our experiments we used micromolar protein concentration. Hence, molecular crowding may have affected protein diffusion by slowing the molecular motion. However, the rationale of using micromolar concentration was necessitated by the need to resemble the real-life situation where the drug delivery vehicle should be able to carry a high load of bioactive molecules. In the literature, solution diffusivity values of  $\approx 1.04, 0.9, 0.6,$  and  $0.4 \times 10^{-10} \text{ m}^2 \text{ s}^{-1}$  for lysozyme, soybean trypsin inhibitor, BSA, and IgG, respectively, have been reported at infinitely dilute conditions at 20 °C (11–14). The diffusion coefficients of freshly prepared protein solutions using FCS analysis were similar to those calculated for the same proteins after release through the hydrogel. This result suggests that the interaction of the proteins with the nanofiber hydrogel did not induce changes in the protein size as a result of unfolding and/or aggregation.

Application of the commonly used Fickian model, which is described by Eq. 2 (see *Materials and Methods*), resulted in apparent protein diffusion coefficients inside the hydrogel, which significantly differed from those of the proteins in solution (up to  $\approx 80\%$ ). The model was developed assuming diffusion of small molecules, infinite dilution of the diffusant, and that the diffusion of the molecules through the hydrogel depends solely on Brownian motion. Eq. 2 is commonly used to determine apparent diffusion coefficients even when these conditions do not apply. The reason for doing so is that it facilitates the discussion of systems when there is no other easily transferable method for determining the diffusivity. In hydrogel systems, these assumptions are rarely satisfied, and therefore, it was expected that the calculated apparent protein diffusion coefficients from Eq. 2 would differ from those determined inside the



**Table 1. Protein properties and diffusion constants using the Stokes-Einstein equation and FCS analysis (Eq. 1)**

Protein	Mol mass, kDa	$r_h$ , nm	pI	Diffusion constants of proteins ( $10^{-10}$ m <sup>2</sup> /s)				
				Stokes-Einstein estimate	Native in PBS (FCS analysis)	Released in PBS (FCS analysis)	Apparent in gel (Eq. 2)	Pristine in gel (FCS analysis)
Lysozyme	14.3	1.9	11.4	1.15	$0.97 \pm 0.18$	$0.96 \pm 0.24$	$0.50 \pm 0.02$	$0.71 \pm 0.05$
Trypsin inhibitor	20.1	2.4	4.6	0.91	$0.74 \pm 0.14$	$0.72 \pm 0.18$	$0.32 \pm 0.01$	$0.61 \pm 0.04$
BSA	66.0	3.6	5.3	0.61	$0.53 \pm 0.10$	$0.51 \pm 0.12$	$0.24 \pm 0.02$	$0.41 \pm 0.06$
IgG	$\approx 150.0$	5.3	$\approx 7.2$	0.40	$0.38 \pm 0.08$	$0.40 \pm 0.09$	$0.07 \pm 0.01$	$0.28 \pm 0.02$

Diffusion constants inside the hydrogel were estimated using Eq. 2 (apparent) and Eq. 1 (pristine). SD values were calculated using error propagation ( $n = 4$  or  $n = 8$ ).

hydrogel using the FCS single-molecule analysis. Plotting the release data as a function of the square root of time (Fig. 2 *Inset*) showed that the diffusion mechanism is biphasic. The initial linear part of each plot indicates diffusion controlled release of the proteins through the peptide hydrogel, and it is used to calculate diffusion coefficients based on Fick's law (Eq. 2) (15, 16). Deviation from the straight line at longer times may be associated with non-Fickian, anomalous diffusion. Hydrogel pores with small sizes and/or diffusion hindrance caused by specific interactions between diffusing protein molecules and peptide nanofibers of the hydrogel may also account for the deviation from Fick's law.

The peptide hydrogel consists of  $\approx 99\%$  (wt/vol) water, and large water voids exist within the hydrogel matrix. Therefore, it is not surprising that the difference between the FCS-determined diffusion coefficients of the proteins in solution and inside the hydrogel is small, i.e., between 18 and 30% (Table 1). However, single-molecule analysis inside the hydrogel obtained diffusivity values for freely moving protein particles. Protein molecules that may be closely interacting with the peptide nanofibers of the hydrogel could not be directly detected, although it may be argued that this interaction would most likely be negligible because of a lack of charge effects between proteins and nanofibers.

**Effect of Peptide Hydrogel Density on Protein Diffusion.** To investigate the effect of the hydrogel density on the release profiles of the proteins, we varied the self-assembling peptide concentrations. Increasing the peptide concentration resulted in a higher density network of nanofibers that could hinder the release of the proteins. In Fig. 3, the release profiles of lysozyme and IgG are plotted upon diffusion through hydrogels with peptide concentrations of 0.5% (wt/vol) (99.5% water), 1.0% (wt/vol) (99% water), and 1.5% (wt/vol) (98.5% water). The results show that protein release through the hydrogel is efficiently controlled upon varying the peptide nanofiber density.

**Conformational Properties of Released Proteins.** Protein aggregation events and protein-peptide interactions resulting in protein inactivation could occur during the protein's residence in the peptide solution, during self-assembly and nanofiber formation, or during the release process. Protein denaturation followed by unfolding or aggregation is expected to influence the diffusivity values. To determine whether this event had occurred, the native and released protein diffusivities were determined by using FCS method. Data analysis showed that the diffusivity values of the released proteins were similar to that of the native proteins (Table 1), which suggests that the proteins did not unfold or aggregate during interaction with the hydrogel system. To obtain further insight into the conformational state of the released proteins, far-UV CD and fluorescence spectroscopy were used to examine the secondary and tertiary structural characteristics, respectively.

CD spectra of the native proteins were nearly identical to those reported in the literature for lysozyme (17), trypsin inhibitor (18), BSA (19), and IgG (20). As may be seen in Fig. 4, the CD spectra of the released proteins closely resembled those of the proteins in the native state. Small deviations were observed in some spectra at wavelengths  $< 200$  nm where the diode or HT (i.e., total absorption) level was high. The relatively low concentration of released proteins, in conjunction with the possible presence of detached nanofibers from the scaffold, could be reasons for the low signal-to-noise ratio observed in this region of the spectrum. However, in the case of released IgG, the  $\beta$ -sheet content of the protein, as seen from the 218-nm ellipticity, was not affected during the release process.

Fluorescence emission spectra were recorded with excitation at 300 nm to excite the tryptophans: the emission spectrum is sensitive to the tryptophan microenvironment within the 3D structure of the protein, and therefore, the spectra can be used to detect tertiary structure changes of the proteins upon release through the hydrogel. The fluorescence spectra of the proteins studied in this work were in line with literature reports recorded at the same experimental conditions for lysozyme (21), trypsin inhibitor (22), BSA (23), and IgG (24). The emission spectra of all released proteins were similar to those of the native proteins with respect to both the emission maximum and fluorescence intensity after normalization for the concentration (Fig. 5).

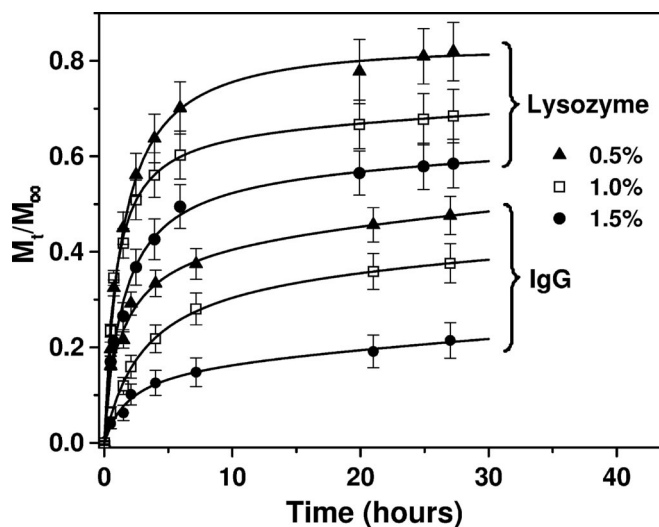


**Fig. 3.** Release profiles for lysozyme and IgG through hydrogels of different peptide nanofiber densities. Hydrogels consisted of self-assembling peptide Ac-(RADA)<sub>4</sub>-CONH<sub>2</sub> with concentrations of 0.5% wt/vol ( $\blacktriangle$ ), 1.0% wt/vol ( $\square$ ), and 1.5% wt/vol ( $\bullet$ ). Release experiments were performed in PBS (pH 7.4) at room temperature. Data points represent the average of 5 samples with calculated SD  $< 12\%$ .

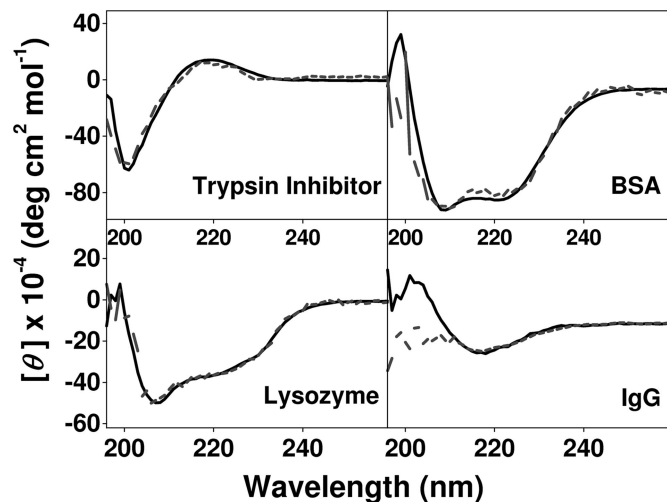


Fig. 4. Far-UV CD spectra of native (solid line) and released (broken line) protein solutions through the peptide hydrogel in PBS (pH 7.4). Spectra were recorded at room temperature.

**Functionality Assays of Released Proteins.** Although many studies characterize protein release kinetics, there is an apparent dearth in the literature of proving functionality after release. By using the *Micrococcus lysodeikticus* cell membrane hydrolysis assay, released lysozyme yielded an activity of  $\approx 102$  substrate units/mg of lysozyme in the reaction solution. This activity level was essentially identical to that measured when freshly prepared lysozyme solutions interacted with the reaction solution. Therefore, lysozyme functionality was not affected upon incorporation and release through the hydrogel.

In the case of trypsin inhibitor, trypsin activity was determined with and without the addition of released trypsin inhibitor. It was observed that uninhibited trypsin had a normalized activity (in substrate units/mg of enzyme) of  $\approx 6,100$ . Upon addition of hydrogel-released trypsin inhibitor, the activity of 1.5 and 3 mg/L trypsin in the reaction mixture was reduced to 0 and 2,210, respectively, which shows that hydrogel-released trypsin inhibitor was active and could fully suppress the activity of 1.5 mg/L

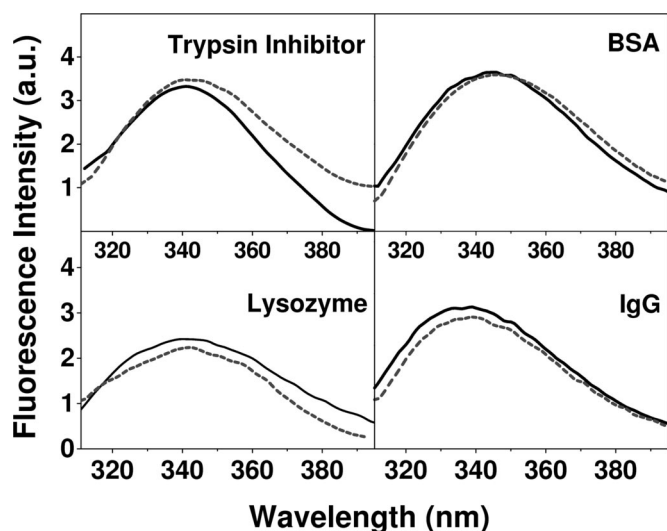


Fig. 5. Normalized fluorescence emission spectra of the native (solid line) and released proteins (broken line) through the peptide hydrogel in PBS (pH 7.4). Spectra were recorded at room temperature; the excitation wavelength was 300 nm.

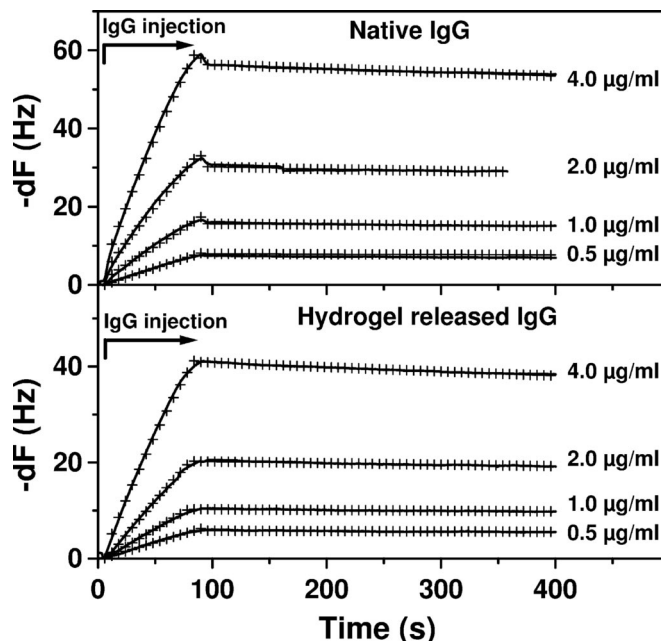


Fig. 6. QCM time-dependent frequency changes,  $-dF$ , upon association (binding) and dissociation of the monoclonal anti-rhodopsin IgG to immobilized rhodopsin (antigen) with different concentrations of IgG. Time 0 represents injection of IgG in the flow channel (kinetic data were shifted for comparison). Arrow indicates the antibody injection time course and the corresponding association phase. The biosensor signal (solid line) increases upon IgG injection and decreases upon injection of the buffer, which rinses the surface and dissociates the IgG bound to the antigen. The similarity of the calculated rate constants and of the affinity constants suggests that the functional characteristics of IgG were not affected upon release through the peptide hydrogel. Global fitting of the binding data are represented by the cross-mark lines.

trypsin in the reaction solution. Similar activity values were obtained when freshly prepared trypsin inhibitor solutions were used.

The functionality of the released BSA was not tested because of the lack of an assay that provides conclusive data; the lack of secondary or tertiary structure perturbations after release suggests conservation of protein biochemical characteristics.

To test the functionality of IgG (monoclonal against the native C terminus of the transmembrane protein bovine rhodopsin) before and after being released through the peptide hydrogel, we used the quartz crystal microbalance (QCM) technique. Criteria for IgG functionality were the kinetics of binding and the affinity constants between the monoclonal IgG and rhodopsin (antigen). Upon interaction with rhodopsin immobilized on the gold surface of the QCM it was shown that after 48 h in the peptide hydrogel, the released anti-rhodopsin IgG did not undergo functional changes compared with the native anti-rhodopsin IgG. Upon fitting of the data in Fig. 6, the kinetic analysis showed that the association  $k_a = 1.69 \pm 0.23 \times 10^6 \text{ M}^{-1} \text{ s}^{-1}$  and dissociation  $k_d = 3.31 \pm 0.65 \times 10^{-4} \text{ s}^{-1}$  rate constants for the native IgG were similar to those observed for the hydrogel-released IgG  $k_a = 1.34 \pm 0.28 \times 10^6 \text{ M}^{-1} \text{ s}^{-1}$ ,  $k_d = 4.66 \pm 0.13 \times 10^{-4} \text{ s}^{-1}$ . Furthermore, the binding constants, defined as  $K_d = k_d/k_a$ ,  $K_d = 0.20 \text{ nM}$  and  $K_d = 0.35 \text{ nM}$  for the native and released IgG, respectively, were similar.

## Conclusions

Designer self-assembling peptide hydrogel scaffolds have the potential to be a robust system for sustained-release applications. The peptide solution mixed with proteins that have therapeutic properties may be applied into a specific tissue and

release its load locally over time. In this work, we showed that proteins with different molecular mass, isoelectric points, and morphologies were released slowly through the Ac-(RADA)<sub>4</sub>-CONH<sub>2</sub> peptide hydrogel. Protein release through this hydrogel depended on the protein size and the density of the peptide nanofibers. We determined by single-molecule FCS analysis the pristine in-gel diffusion coefficients of the proteins, and we showed that application of commonly used Fickian diffusion models underestimate the in-gel diffusion coefficients of proteins.

An efficient controlled release system should yield biologically active proteins. We tested the released proteins and found that encapsulation and release did not affect the secondary and tertiary structure of the proteins studied, nor was their functionality diminished. These results lay the foundation for creating new designer, tailor-made peptide hydrogels for controlled release of proteins. Peptide hydrogels can be easily designed and synthesized to control the release of proteins and other therapeutic compounds by varying the density of the nanofibers of the hydrogel or by changing the charge of the nanofibers simply by adding amino acids with positively or negatively charged side groups. Overall, this system would allow the release of diffusing molecules in a sustainable and highly efficient way. We anticipate that further fine-tuned systems will have a wide range of applications not only for biomedical technology but also for clinical treatment of a number of diseases that required sustained releases of therapeutically active proteins.

## Materials and Methods

**Chemicals and Reagents.** The Ac-(RADA)<sub>4</sub>-CONH<sub>2</sub> peptide in 1% solution was obtained from Puramatrix and in powder from CPC Scientific. Chicken egg white lysozyme, soybean trypsin inhibitor, and BSA were purchased from Sigma–Aldrich. Monoclonal IgG (Cell Essentials), which is specific for the 1D4 (TETSQVAPA-COOH) sequence at the C terminus of native bovine rhodopsin (25), was purified by gel filtration to >95% as determined by SDS/PAGE. The pI of anti-rhodopsin IgG was 6.7 as determined by isoelectric focusing. To detect the protein molecules with the fluorescence single-molecule technique, labeling was conducted by using the Alexa Fluor 647 microscale protein-labeling kit (Molecular Probes). Labeled proteins were purified, and the unreacted dye molecules were removed by gel filtration.

**Protein Release Experiments.** Peptide hydrogels were formed by using well-established protocols (5–7, 10). Briefly, the Ac-(RADA)<sub>4</sub>-CONH<sub>2</sub> peptide solution was mixed with PBS (pH 7.4) containing both labeled and unlabeled protein at a final concentration of 5 nM and 5 μM, respectively. Forty microliters of the mixture was transferred into the wells of a 384-well plate, and gelation occurred within 15 min. Subsequently, 70 μL of PBS was slowly added to the 40 μL of the hydrogel. To satisfy the perfect-sink conditions and allow for the determination of the protein release profile, 40 μL of the supernatant was replaced with the same volume of fresh PBS at frequent time points. During the course of the measurements the hydrogel volume did not change, and therefore protein release could not be attributed to hydrogel degradation or swelling. Preliminary experiments did not show any detectable adsorption of trypsin inhibitor, BSA, and IgG on the surface of the 384-well plates. Small adsorption of lysozyme on the borosilicate glass of the wells was prevented by pretreatment and blocking of the wells with 3% nonlabeled BSA, overnight incubation at 37 °C, and thorough washing of the wells to remove unbound BSA. Blocking prevented lysozyme adsorption.

**Protein Concentration and Diffusivities from FCS Single-Molecule Analysis.** FCS characterization of the protein–hydrogel system was performed at room temperature by using the FluoroPoint single-molecule detection system (Olympus). Alexa Fluor 647 fluorescently labeled protein molecules crossing the confocal femtoliter volume were excited with a He-Ne laser at 633 nm. Protein concentrations in the supernatant and inside the hydrogel were determined by using the FluoroPoint FCS system. The number of the Alexa Fluor 647-labeled protein molecules crossing the confocal volume (counts per unit time) was measured and converted to concentration by using a calibration curve of the respective fluorescently labeled protein at different concentrations.

Fluctuations in fluorescent intensity within a confocal volume are recorded as a function of time, and the autocorrelation function,  $g(\tau)$  is influenced by the properties of the fluorescing molecules and the diffusion dynamics in the local environment (26, 27). Although several expressions have been developed

to define the autocorrelation function for the case of anomalous 3D diffusion of monodisperse particles in solution (26, 28–30), the FluoroPoint system used Eq. 1

$$g(\tau) = 1 + \left( \frac{1 - F_{\text{trip}} + F_{\text{trip}}e^{-\tau/\tau_{\text{trip}}}}{N} \right) \left( \frac{1}{1 + (\tau/\tau_D)} \right) \left( \frac{1}{1 + (1/s^2)(\tau/\tau_D)} \right)^{\frac{1}{2}} \quad [1]$$

where  $g(\tau)$  is a function of the fractional population ( $F_{\text{trip}}$ ) and decay time ( $\tau_{\text{trip}}$ ) of the triplet state,  $N$  is the number of molecules within the sample volume,  $\tau_D$  is the translational diffusion time, and  $s$  is a factor describing the cylindrically shaped detection volume and is equal to the ratio of the radius of the cylinder's basal plane ( $\omega_0$ ) divided by one-half of its height ( $\omega_1$ ). In a fully anisotropic solution, with diffusing molecules significantly smaller than the confocal volume, the diffusion coefficient  $D$  of the molecules (e.g., protein) is equal to  $D = \omega_0^2/4\tau_D$ . The autocorrelation profile was fit by using single and multiple translational diffusion times, and in all cases it was adequately described by a single  $\tau_D$ . The goodness of fit for each dataset was judged by the value of the  $\chi^2$  parameter and by inspection of the residuals, which were distributed uniformly around zero. Attempted fits to a model with more independent components did not result in smaller  $\chi^2$  values.

The diffusion of the protein molecules was monitored in both the hydrogel and the supernatant samples, which were removed at different time points. For the FCS calculation of the diffusion coefficients in solution, 4–10 measurements of  $D$  were recorded for each supernatant sample, averaged, and SD values were calculated. The pristine, inside the hydrogel, diffusion coefficients were measured for each protein in the hydrogel at every time point a supernatant sample was taken and averaged throughout the series of measurements. All data points represent the average of 4 or 8 samples. Uncertainties in the calculated parameters were estimated via common error propagation techniques: for a function  $y = g(x_1, x_2)$ , errors in the calculated values were determined by using the relationship  $\sigma_y^2 = (\partial g/\partial x_1)^2 \sigma_{x_1}^2 + (\partial g/\partial x_2)^2 \sigma_{x_2}^2$ .

**Diffusivity Determination from Released Protein Concentration.** For a hydrogel matrix that contains a molecularly dispersed diffusing agent, the apparent diffusion coefficient may be calculated by using the 1D unsteady-state form of Fick's second law of diffusion, which for small values of time ( $t$ ) is given by (10, 15, 16):

$$\frac{M_t}{M_\infty} = \left( \frac{16 D_{\text{app}} t}{\pi H^2} \right)^{0.5} \quad [2]$$

where  $D_{\text{app}}$  is the apparent diffusivity,  $M_t$  and  $M_\infty$  are the cumulative mass of the diffusing compound released from the hydrogel after  $t$  and infinite time ( $\infty$ ), respectively. The thickness of the hydrogel matrix ( $H$ ) inside the well was calculated from the volume of the peptide–protein solution (i.e., 40 μL) and from the dimensions of the wells of the 384-well plate.  $D_{\text{app}}$  may be obtained from the slope of the straight line fitting the data of  $M_t/M_\infty$  vs.  $t^{0.5}$ , for  $0 < M_t/M_\infty < 0.6$ .

**Diffusivity from Stokes–Einstein equation.** For isolated particles that follow a Brownian motion in a medium, the diffusion coefficient may be calculated by the Stokes–Einstein equation  $D_{S-E} = k_B T/6\pi\eta r_h$ , where  $k_B$  is the Boltzmann constant,  $T$  is the absolute temperature of the medium,  $\eta$  is the dynamic viscosity of the solvent (taken as 1.002 cP), and  $r_h$  is the hydrodynamic radius of the protein obtained from the literature for lysozyme (31), trypsin inhibitor (32), BSA (33), and IgG (34) (Table 1).

**CD.** Far-UV CD spectra were recorded between 190 and 260 nm at room temperature on an Aviv 62DS spectrometer. CD spectra of proteins released from the hydrogel after 12 h of diffusion were compared with those of freshly prepared protein solutions at concentrations corresponding to the protein concentration after 12-h release. Spectra were recorded in 1-nm steps and averaged over 2 s. All measurements were carried out in 1-mm quartz cuvettes in PBS (pH 7.4). Spectra resulted from accumulation of 4 scans that were averaged. Blank spectra of the buffer without protein, obtained under identical conditions, were subtracted.

**Fluorescence Emission Spectroscopy.** Fluorescence emission of released and native proteins was measured by using a PerkinElmer LS-50B spectrophotometer at room temperature with quartz cuvettes of 1-cm path length. Emission spectra were recorded between 310 and 400 nm on excitation at 300 nm. The



excitation and emission slit widths were set at 5.0 and 2.5 nm, respectively. Sample conditions were identical to those described for the CD measurements. All spectra were corrected for the background emission of water.

**Protein Functionality Assays.** Lysozyme and trypsin inhibitor activity was determined by using the respective protein assay kits (Sigma–Aldrich). Normalized lysozyme activity (substrate units per mg of enzyme) was determined by using an assay that is based on the hydrolysis of the outer cell membrane of *M. lysodeikticus* (35). Samples of native and hydrogel-released lysozyme were mixed with the *M. lysodeikticus* suspension in 66 mM phosphate buffer (pH 6.2), and the decrease in turbidity was measured for 3 min at 450 nm. The activity of the hydrogel-released lysozyme was compared with native lysozyme to confirm functionality of the released protein.

The normalized trypsin activity (substrate units per mg of enzyme) was determined by using a series of 3.2-mL reaction mixture solutions comprising 63 mM PBS, 0.23 mM *N*-benzoyl-L-arginine ethyl ester, 0.002 mM HCl, and 0.005–0.01 mg of trypsin. Suppression of trypsin activity caused by the addition of hydrogel-released trypsin inhibitor was compared with freshly prepared control trypsin inhibitor solutions.

The functionality of native and hydrogel-released anti-rhodopsin monoclonal IgG was assayed by QCM (A100 C-Fast system; Attana). The setup consists of a thin piezoelectric quartz disc having electrodes on each side. When connected to an oscillating current, the quartz crystal oscillates at resonant frequencies that are sensitive to the crystal mass; as material adsorbs to the surface of the crystal the recorded frequency changes. To test the binding properties of the hydrogel-released anti-rhodopsin IgG we covalently immobilized rhodopsin (antigen) to the carboxyl-modified gold surface of the

QCM by using an amine coupling kit (Attana) according to instructions provided with the kit and compared the binding affinity of native IgG with that of the hydrogel-released IgG. Preliminary experiments showed that nonspecific binding was minimal in 0.05% Tween detergent, and therefore all IgG–antigen binding studies were performed at this Tween concentration.

The temperature of the QCM cell was 22 °C controlled by a Peltier element. Between each measurement, the surface was regenerated by a 20-s pulse of 8  $\mu$ L of 10 mM NaOH. Kinetic data were obtained by injecting 35  $\mu$ L of 0.5, 1, 2, or 4  $\mu$ g/mL anti-rhodopsin IgG for 84 s at 25  $\mu$ L/min flow rate over a rhodopsin-coated surface and measuring the mass increase of the surface caused by IgG binding to rhodopsin. Buffer was injected before and after each concentration series and used as reference. The kinetic data were corrected for negative controls, which consist of the signals observed upon injecting (i) anti-rhodopsin IgG over a surface with immobilized BSA and (ii) a polyclonal IgG over the surface with immobilized rhodopsin. The data were analyzed by using the ClampXP software and modeled for the binding reaction event between the antibody and the antigen that was mass transport limited to account for the diffusion of the antibody inside the microfluidic device of the QCM cell (36). From the analysis we calculated the  $K_a$  and  $k_d$  rate constants and the  $K_d$  values of the native and released IgG for the antigen. The fitting was evaluated based on the  $\chi^2$  value and the residual error that was near zero.

**ACKNOWLEDGMENTS.** We thank Dr. Daniel Oprian (Brandeis University, Waltham, MA) for the gift of bovine rhodopsin and Dr. Liselotte Kaiser (Attana AB, Stockholm, Sweden) for technical support with the QCM system. This work was supported in part by National Institutes of Health Grant BRP EB003805 (to S.Z.). S.K. is a HighQ Foundation Fellow. Y.N. was supported by Menicon Co., Ltd., Japan.

- Hoffman AS (2002) Hydrogels for biomedical applications. *Adv Drug Deliv Rev* 54:3–12.
- Hou Q, De Bank PA, Shakesheff KM (2004) Injectable scaffolds for tissue regeneration. *J Mater Chem* 14:1915–1923.
- Elisseff J (2004) Injectable cartilage tissue engineering. *Expert Opin Biol Theor* 4:1849–1859.
- Drury JL, Mooney DJ (2003) Hydrogels for tissue engineering: Scaffold design variables and applications. *Biomaterials* 24:4337–4351.
- Zhang SG, Holmes T, Lockshin C, Rich A (1993) Spontaneous assembly of a self-complementary oligopeptide to form a stable macroscopic membrane. *Proc Natl Acad Sci USA* 90:3334–3338.
- Kisiday J, et al. (2002) Self-assembling peptide hydrogel fosters chondrocyte extracellular matrix production and cell division implications for cartilage tissue repair. *Proc Natl Acad Sci USA* 99:9996–10001.
- Narmonova D, et al. (2005) Self-assembling short oligopeptides and the promotion of angiogenesis. *Biomaterials* 26:4837–4846.
- Davis ME, et al. (2005) Injectable self-assembling peptide nanofibers create intramyocardial microenvironments for endothelial cells. *Circulation* 111:442–450.
- Ellis-Behnke RG, et al. (2006) Nano neuro knitting: Peptide nanofiber scaffold for brain repair and axon regeneration with functional return of vision. *Proc Natl Acad Sci USA* 103:5054–5059.
- Nagai Y, Unsworth LD, Koutsopoulos S, Zhang S (2006) Slow release of molecules in self-assembling peptide nanofiber scaffold. *J Control Rel* 115:18–25.
- Smith MH (1970) in *Handbook of Biochemistry*, ed Sober HA (Chemical Rubber Company, Cleveland, OH), 2nd Ed, pp C3–C35.
- Merrill EW, Dennison KA, Sung C (1993) Partitioning and diffusion of solutes in hydrogels of poly(ethylene oxide). *Biomaterials* 14:1117–1126.
- Walthers RR, Graham JF, Moore RM, Anderson DJ (1984) Protein diffusion coefficient measurements by laminar flow analysis: Method and applications. *Anal Biochem* 14:190–195.
- Burczak K, Fujisato T, Hatada M, Ikada Y (1994) Protein permeation through poly(vinyl alcohol) hydrogel membranes. *Biomaterials* 15:231–238.
- Crank J, Park GS (1968) *Diffusion in Polymers* (Academic, NY).
- Higuchi T (1963) Mechanism of sustained-action medication. Theoretical analysis of rate of release of solid drugs dispersed in solid matrices. *J Pharm Sci* 52:1145–1149.
- Halper JP, Latovitzki N, Bernstein H, Beychok S (1971) Optical activity of human lysozyme. *Proc Natl Acad Sci USA* 68:517–522.
- Roychaudhuri R, Sarath G, Zeece M, Markwell J (2003) Reversible denaturation of the soybean Kunitz trypsin inhibitor. *Arch Biochem Biophys* 412:20–26.
- Kondo A, Murakami F, Higashitani K (1992) Circular-dichroism studies on conformational changes in protein molecules upon adsorption on ultrafine polystyrene particles. *Biotechnol Bioeng* 40:889–894.
- Ikeda K, Hamaguchi K, Migita S (1968) Circular dichroism of Bence–Jones proteins and immunoglobulins G. *J Biochem* 63:654–660.
- Acharya AS, Taniuchi H (1978) Reduction and renaturation of hen egg lysozyme containing carboxymethylcysteine-6 and -127. *Biochemistry* 17:3064–3070.
- Ishida M, Hamaguchi K, Ikenaka T (1970) A study on the interaction of soybean trypsin inhibitor with trypsin by circular dichroism. *J Biochem* 67:363–371.
- Zhang F, Thottananiyil M, Martin DL, Chen C-H (1999) Conformational alteration in serum albumin as a carrier for pyridoxal phosphate: A distinction from pyridoxal phosphate-dependent glutamate decarboxylase. *Arch Biochem Biophys* 364:195–202.
- Nishiyama Y, et al. (2005) Broadly distributed nucleophilic reactivity of proteins coordinated with specific ligand binding activity. *J Mol Recognit* 18:295–306.
- Molday RS, MacKenzie D (1983) Monoclonal antibodies to rhodopsin: Characterization, cross-reactivity, and application as structural probes. *Biochemistry* 22:653–660.
- Rigler R, Elson ES (2001) *Fluorescence Correlation Spectroscopy: Theory and Applications* (Springer, New York).
- Webb WW (2001) Fluorescence correlation spectroscopy: Inception, biophysical experiments, and prospectus. *Appl Opt* 40:3969–3983.
- Saxton MJ (1994) Anomalous diffusion due to obstacles: A Monte Carlo study. *Biophys J* 66:394–401.
- Saxton MJ (1996) Anomalous diffusion due to binding: A Monte Carlo study. *Biophys J* 70:1250–1262.
- Krichesky O, Bonnet G (2002) Fluorescence correlation spectroscopy: The technique and its applications. *Rep Prog Phys* 65:251–297.
- Brown RGW, Burnett JG, Mansbridge J, Moir CI (1990) Miniature laser-light scattering instrumentation for particle-size analysis. *Appl Opt* 29:4159–4169.
- Leach BS, Fish WW (1977) Resistance of soybean trypsin inhibitor (Kunitz) to denaturation by guanidinium chloride. *J Biol Chem* 252:5239–5243.
- Tanford C, Buzzell JG, Rands DG, Swanson SA (1955) The reversible expansion of bovine serum albumin in acid solutions. *J Am Chem Soc* 77:6421–6428.
- Armstrong JK, Wenby RB, Meiselman HJ, Fisher TC (2004) The hydrodynamic radii of macromolecules and their effect on red blood cell aggregation. *Biophys J* 87:4259–4270.
- Shugar D (1952) The measurement of lysozyme activity and the ultraviolet inactivation of lysozyme. *Biochim Biophys Acta* 8:302–309.
- Myszka DG, Morton TA, Doyle ML, Chaiken IM (1997) Kinetic analysis of a protein antigen–antibody interaction limited by mass transport on an optical biosensor. *Biophys Chem* 64:127–137.
- Malcolm BA, Wilson KP, Matthews BW, Kirsch JF, Wilson AC (1990) Ancestral lysozymes reconstructed, neutrality tested, and thermostability linked to hydrocarbon packing. *Nature* 345:86–89.
- Song HK, Suh SW (1998) Kunitz-type soybean trypsin inhibitor revisited: Refined structure of its complex with porcine trypsin reveals an insight into the interaction between a homologous inhibitor from *Erythrina caffra* and tissue-type plasminogen activator. *J Mol Biol* 275:347–363.
- Bhattacharya AA, Curry S, Franks NP (2000) Binding of the general anesthetics propofol and halothane to human serum albumin: High-resolution crystal structures. *J Biol Chem* 275:38731–38738.
- Harris LJ, et al. (1992) The three-dimensional structure of an intact monoclonal antibody for canine lymphoma. *Nature* 360:369–372.